

# Aerodynamic Design Studies of a Transonic Centrifugal Compressor Impeller Based on Automated 3D-CFD Optimization

T. Raitor, O. Reutter, M. Aulich, E. Nicke

German Aerospace Center DLR, Institute of Propulsion Technology,  
Linder Hoehe, 51147 Cologne, Germany  
till.raitor@dlr.de, oliver.reutter@dlr.de, marcel.aulich@dlr.de, eberhard.nicke@dlr.de

## ABSTRACT

A transonic centrifugal compressor is optimized to improve the performance of the impeller by varying the geometry of blades and the meridional contour in the axial range of the main blades. The main objectives are to increase the isentropic efficiency and the operating range. A genetic algorithm controlling an automated process chain is used as the optimization method.

To ensure a wide operating range the optimization is performed at three operating points on the 100 % speed line. A method, which is developed to use stationary CFD calculations for predicting the blade tone noise, the strongest component of the compressor noise, is used to reduce the compressor noise emissions.

To evaluate the success of the optimization their best members' fitness values will be analyzed experimentally.

The optimization procedure is described in detail. The geometrical modifications leading to the aerodynamic and acoustic improvements are discussed. A mechanical stress optimization of the impeller is planned for the near future.

## NOMENCLATURE

BPF	blade passing frequency	$k$	specific turbulent kinetic energy
CFD	computational fluid dynamics	$Ma_{isen}$	isentropic Mach number
CNC	computer numerical control	$\dot{m}$	mass flow
CSM	Cumpsty margin, modified form of the stall margin	$m'$	specific length
DLR	Deutsches Zentrum für Luft- und Raumfahrt (German Aerospace Center)	$p_{st}$	static pressure
MB	main blade	$r_{LE}$	radius of the leading edge
OP	operating point	$r_{TE}$	radius of the trailing edge
RANS	Reynolds-averaged Navier-Stokes	$t$	time
SB	splitter blade	$T$	cycle duration; time for one impeller revolution
SRV	type series of centrifugal compressors developed at DLR: “ <i>schnell laufender Radialverdichter</i> ” (fast running centrifugal compressor)	$x/c$	relative chord length
S2	meridional plane in turbomachines	$y^+$	distance wall coordinate
TRACE	Turbomachinery Research Aerodynamic Computational Environment (flow solver)	$\beta_{LE}$	angle of the leading edge
		$\beta_{ST}$	stagger angle
		$\beta_{TE}$	angle of the trailing edge
		$\Theta$	circumferential angle
		$\Pi_{tt}$	total pressure ratio of the stage
		$\eta_{isen}$	isentropic efficiency
		$\omega$	specific dissipation rate

## INTRODUCTION

Centrifugal compressors are applied where high pressure ratios at relative low mass flow rates compared to axial compressors and a compact architecture are necessary, for example in turbocharging diesel engines in large ships or power stations, in cooling and gas transportation systems in the chemical industry (Persigehl et al. 2011) or in small aircraft engines. An increasing field of application of centrifugal compressors are in devices for more efficient carbon capture in powerstations with reduced carbon dioxide emissions.

The growing demand for higher engine power output and small ecological impact requires high efficient low noise compressors with smaller construction volumes but high aerodynamic performance (Casey and Gersbach 2008 and Van den Braembussche 2000).

Automated optimizers are increasingly used in order to improve radial compressors. Yagi et al. (2010) optimized the suction channel to improve the efficiency of process centrifugal compressor. Van den Braembussche et al. (2012) introduced a multidisciplinary multipoint optimization procedure in order to improve the efficiency in the design point and the operating range of a transonic turbocharger compressor.

The main goals of the performance optimization of a transonic centrifugal compressor described here are the enhancement of the isentropic efficiency and the operating range. To ensure the second objective, three operating points on the 100 % speed line are implemented into the optimization process chain.

Earlier studies showed that the main noise component of transonic centrifugal compressors, the shock induced blade tone noise (Raitor 2010), and the isentropic efficiency are both dependent on the preshock Mach number and the shock position relative to the blade chord. So it is sufficient to use only the isentropic efficiency as an objective.

The previous members of the SRV series, including the SRV4 (Krain and Hoffmann, 2005), have been built in flank milling technique, which constrained the design possibilities of the impeller blades and led to limitations in the aerodynamic performance. Modern manufacturing technologies allow 3D-design of the blades leading to a significant increase in the performance and especially the efficiency of the new impellers. So SRV4 (Fig. 4) is the starting point in this study.

For fully 3D-designed blades attention has also to be given to their mechanical stability. A mechanical optimization of the best member of the last optimization run with monitoring the aerodynamic properties is in progress.

In this paper, emphasis is placed on the description of the aerodynamic optimization procedure, the geometrical variations and their influence on the aerodynamic and aeroacoustic behaviour of the centrifugal compressor.

## THE OPTIMIZATION PROCEDURE

### **The Meridional Contour, Blade Generation and Optimization Parameters**

The optimization of the centrifugal compressor described in this paper is performed by the in-house automated optimizer AutoOpti (Siller et al 2009). The first step in the optimization procedure is to parameterize those parts of the turbomachine which need to be varied. Since the best optimization member will be tested experimentally at the DLR test rig some geometrical parameters of the impeller will not be changed. These shall include: the axial length and the diameter at inlet and outlet. Furthermore, the number of the blades will be unchanged. The geometry of the blades and the meridional contour within the axial range of the impeller main blades will be varied at this optimization.

The main and splitter blades of the impeller are optimized independently of each other and are created by an in-house blade generation tool, called BladeGenerator (Siller and Aulich 2010).

All previous impellers have been designed according to the flank milling technique. That means

the blade surfaces of these impellers are ruled surfaces (Krain and Hoffmann 2005). With modern CNC milling machines impellers with 3D blades can be produced. This results in completely new ways to design high performance centrifugal compressors.

The BladeGenerator needs parameterized blade profiles as input so that the blade geometry can easily be changed during the optimization process. For ruling surface blades, two blade profiles are necessary, one at the hub and one at the shroud. For a design of arbitrary surfaces, there can be more. In preliminary studies, it was found that three blade profiles are sufficient to achieve good results in this optimization.

The optimizer needs a minimum of free parameters for a significant geometric variability. The resources increase exponentially over the number of free parameters for a converged optimization phase. It was found that six free parameters for each of the three profiles of the main blade and four control points to shift the leading edge in axial direction (see Fig. 1) are a good compromise between geometric variability of the blades and the need to reduce the free parameters.

These free parameters for each profile are the important angles of the stagger  $\beta_{ST}$ , the leading edge  $\beta_{LE}$  and the trailing edge  $\beta_{TE}$  as well as the radius of the leading edge  $r_{LE}$  and the DeBoor points #3 and #4 on the suction side in  $\Theta$ -direction, which can be seen in Fig.2.

The first and the last DeBoor point are determined by other parameters. They can not be shifted. The second and the next to last point are only movable in  $m'$ -direction. But, in this optimization only a shifting in  $\Theta$ -direction is permitted.

The pressure side is parameterized by a thickness distribution, which will not be varied in this optimization. For more details of the parameterization see Voss and Nicke (2008).

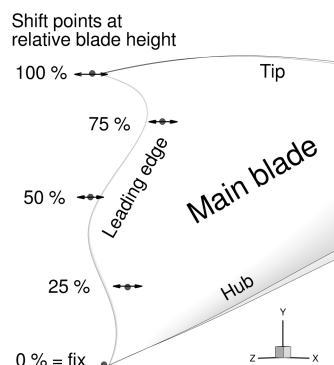


Figure 1: **Shift points of the leading edge (main blade)**

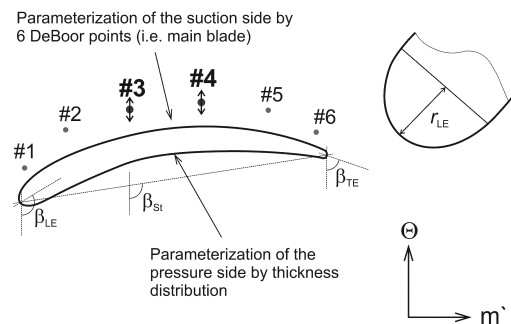


Figure 2: **Parameterization of the blade profile**

The profiles of the splitter blades use the same parameterization as those of the main blades. Only point #3 is needed as a free optimization parameter of the splitter blade profiles. In contrast to the main blade, the splitter blade can be shifted circumferentially by the optimizer and it can change its chord length in a relative wide range while keeping the trailing edge at the same impeller outlet radius as the main blade.

Six free parameters allow a small variation of meridional contour at hub and shroud contour lines.

For the geometrical variation of the impeller the optimization uses all together 45 free parameters.

### Meshing and Flow Simulation of the Compressor Stage

The entire compressor stage consisting of the impeller and a vaneless diffuser is meshed for the flow simulation after the meridional contour and the blades are designed. Figure 3 shows a

compressor passage. The inlet duct and the impeller rotate, the diffuser does not.

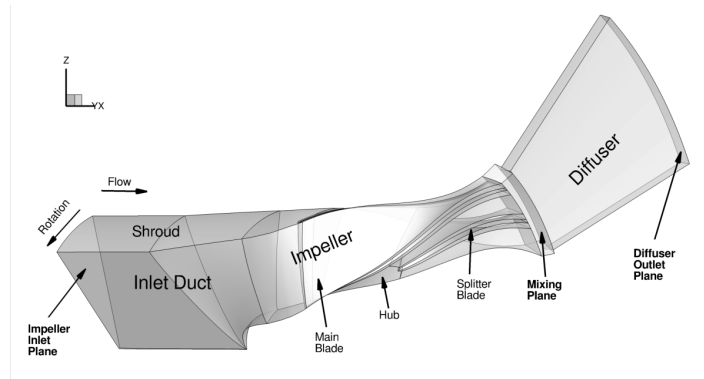


Figure 3: **Passage of the centrifugal compressor stage for the flow simulation**

For this optimization, a structured grid with approximately 910,000 cells with a CH topology is used. The grid is generated for a stationary 3D-RANS simulation using the  $k-\omega$  turbulence model with wall functions. The tip clearances are modelled by separate clearance grids. The flow solver TRACE (Version 7.3, Becker et al. 2010) is used. The  $y^+$  values are in the range of 25 to 50.

Although only the impeller is optimized, the simulation is carried out for the whole stage, comprising the impeller and the diffuser. The mixing plane is located between the impeller exit and the diffuser inlet and the analysis planes are the impeller inlet and the diffuser outlet. The locations of these analysis planes correspond with performance measurement points at the DLR test rig. At the test rig the diffuser continues behind the numerical exit plane and ends in a collection chamber. Fig. 3 shows the passage of the stage which is meshed for the CFD computation.

### The Reference Compressor

Since the aim of this study is to continue the SRV series by using AutoOpti the last impeller of this series, the SRV4, is selected as the initial member. The SRV4 is designed with thirteen flank milled main and thirteen splitter blades. The leading edges of the main blades are swept backward

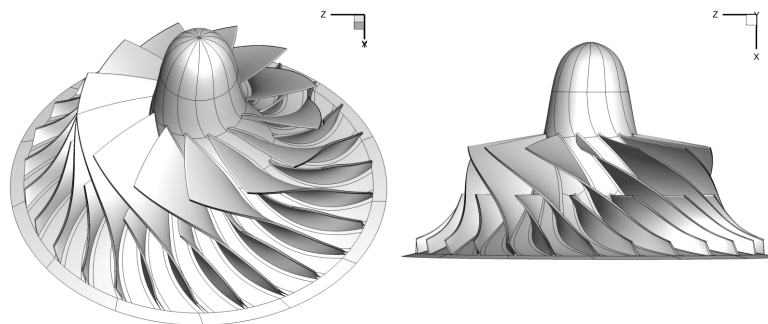


Figure 4: **The impeller SRV4 - the reference member**

by  $9^\circ$ . The splitter blades have no sweep. The trailing edges of both blades are raked by  $15^\circ$  in the direction of rotation. The trailing edge angle  $\beta_{TE}$  of both blades is  $38^\circ$  with respect to the radius. The axial length of the splitter blades is half as long as the main blades. The splitter blades are circumferentially positioned exactly in the middle between two main blades. The reference member SRV4 is described in detail by Krain and Hoffmann (2005).

Some technical specifications must be maintained for the new impellers to ensure the comparability with the previous models and the operability in the test rig. These specifications are the inlet and outlet diameter, the axial length of the impeller and its design speed of 50,000 rpm. Also the number of blades is unchanged because the improvements of the impeller should be achieved rather by a newer way of the blade design and manufacturing than by a different number of blades.

### Optimization Objectives

The goal of the optimization is to improve the aerodynamic performance with the main focus on the efficiency and the operating range of the centrifugal compressor of the DLR series SRV.

At the design speed, where the optimization is performed, three operating points were computed. OP0 is the first operating point at a defined static pressure of 570 kPa at the outlet plane of the stage (diffuser). The first objective (fitness function) is to maximize the isentropic efficiency at OP0. The optimizer AutoOpti always minimizes the fitness functions. Hence, the fitness function is reformulated, so that it can be minimized, therefore it is multiplied by -1.

If the computation is converged, the mass flow rate for the next operating point OP1 will be determined by subtraction of 0.12 kg/s from the mass flow of OP0. After convergence is detected for the computation of OP1 the value of static pressure at the outlet plane of the stage is increased by 2.5 kPa, which defines the static pressure for the last operating point OP2.

The second fitness function evaluates the performance characteristic in the range between OP2 and OP0.

Cumpsty 1989 states for the surge margin:

$$\text{Surge margin} = 1 - \frac{\dot{m}(\text{OP}_{\text{surge}})}{\dot{m}(\text{OP}_{\text{working}})} \cdot \frac{\Pi_{tt}(\text{OP}_{\text{working}})}{\Pi_{tt}(\text{OP}_{\text{surge}})}. \quad (1)$$

For the optimization process a variation of this equation, the CSM (Cumpsty margin), is used:

$$\text{CSM}(\text{OP2}, \text{OP0}) = \frac{\dot{m}(\text{OP0})}{\dot{m}(\text{OP2})} \cdot \frac{\Pi_{tt}(\text{OP2})}{\Pi_{tt}(\text{OP0})}. \quad (2)$$

The operating range is defined from choke to surge. OP0 is defined close to choke of the initial member SRV4. Both other operating points are determined depending on the mass flow rate of OP0 as described above. The distances between the operating points are determined with respect to the operating range of SRV4. It would need a lot of CFD calculations to achieve the numerical surge point, which is not feasible for an optimization. Additionally mass flow controlled CFD computations need a lot more time than pressure controlled ones. This method has been successfully applied at an optimization of an axial compressor stage (Siller et al. 2009).

The first idea to achieve a high mass flow at choke in order to maximize the operating range was not to specify the mass flow rate at OP0. Observations during the optimization run show an increase of the efficiency at higher mass flow rates in OP0. Kriging as surrogate models are used to accelerate the optimization process.

## RESULTS OF THE OPTIMIZATION

### The Pareto Front

Figure 5 shows the fitness values of all converged members of the data base of the optimization. 4138 Members of the data base are converged. The abscissa represents the 2nd objective function CSM(OP2, OP0) (s. Eq. 2) and the ordinate the first objective function, derived from the isentropic efficiency in OP0. As in many optimizations the objective functions are competing. Members with high values of the first fitness function have lower values for the second fitness function and vice versa.

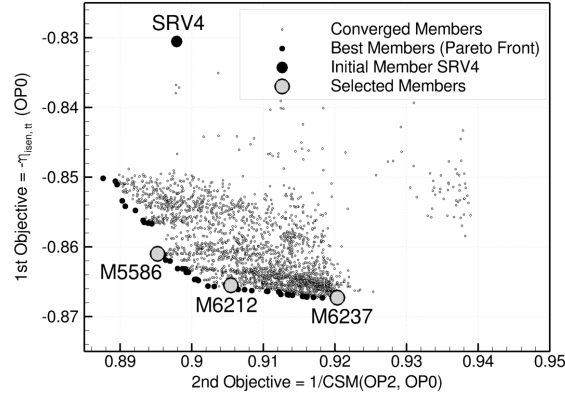


Figure 5: **Plot of the fitness values of all converged members**

The members with the lowest fitness values are the best and form a pareto front which can be seen in Fig. 5. 48 members - marked with black points - belong to the pareto front.

### The Best Members

Three representative members of the pareto front (s. Fig.5) are selected to analyze the optimization and to discuss the results.

The three operating points of the optimization are representative points at the design speed line. The achieved efficiencies at OP0 and the operating ranges (CSM) between OP0 and OP2 are compared to evaluate the success of the optimization (see Table 1, the left columns). Although the impeller is optimized only the efficiency of the whole stage is evaluated in the optimization as a fitness function. In Table 1 the stage and the impeller efficiencies are presented.

In the optimization, member M6237 achieved the highest efficiency for both the impeller and the stage, but the smallest operating range. Member M5586 shows a wider operation range at a lower efficiency. The member M6212 is a compromise between high efficiency and a wide operation range. The differences of the efficiencies between the optimized members are relatively small. All optimized members show an increase of the efficiency compared to the SRV4.

Table 1: **Values of the objectives functions resulting from the optimization procedure compared to those obtained from a completely computed characteristic line at 50,000 rpm.**

Member	optimization results			characteristic line at 50,000 rpm		
	OP0		OP0 - OP2	OP $_{\eta_{max}}$		OP $_{choke}$ - OP $_{surge}$
	$\eta_{isen}$		CSM	$\eta_{isen}$		CSM
	stage	impeller		stage	impeller	
M6237	0.8673	0.9161	1.087	0.8661	0.9149	1.267
M6212	0.8655	0.9145	1.104	0.8659	0.9141	1.248
M5586	0.8611	0.9115	1.117	0.8601	0.9103	1.263
SRV4	0.8305	0.8854	1.114	0.8381	0.8957	1.244

For all of the three selected members a complete characteristic line at 50,000 rpm is computed, shown in Fig. 6. The optimizer shifts the point of the peak efficiency to OP0, because it is an objective to maximize the efficiency in this operating point. But the SRV4 achieved its maximum efficiency at a static pressure at the diffuser outlet of 600 kPa. That is 30 kPa higher than the

static pressure there in OP0. Therefore, it is more realistic to compare the peak efficiencies of the various geometries instead of the efficiencies in an operating point with the same static pressure in the outlet plane. The impeller peak efficiency of M6237 is increased by 1.9 percentage points compared to the SRV4 (Table 1 and Fig. 6b).

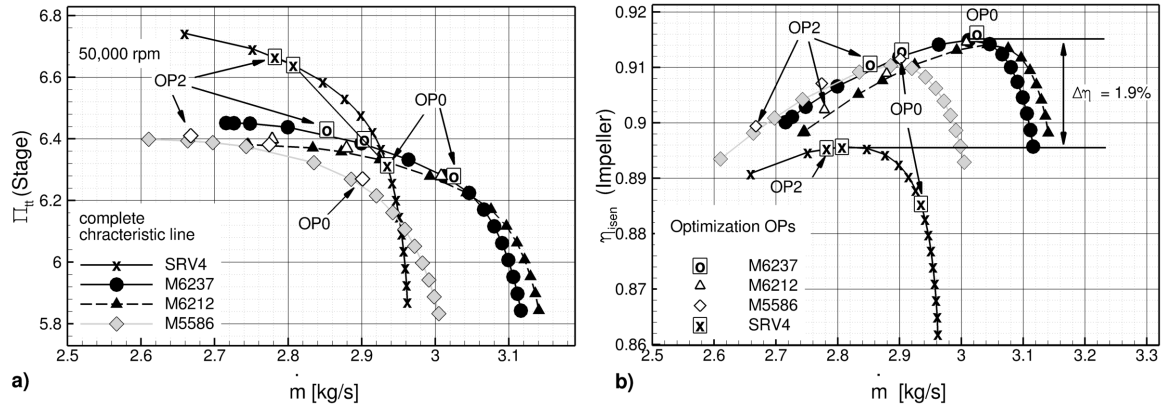


Figure 6: Performance map of the selected best members.

The operation range of the speed line is calculated between first operating point at choke and the last converged point with the lowest mass flow rate, the numerical stability limit. Here the SRV4 shows the widest operation range followed by M6212. The calculated CSM criterion for the last calculated OP and OP0 is given in Table 1. In the optimization process it is not possible to check the surge point of each member. OP2 should be defined at lower mass flow rates in the next optimization to achieve better results for the operating range.

The lower shock losses of the members M6212 and M6237 compared to the SRV4 lead to higher efficiencies. Fig. 7 shows the Mach number distribution and the static pressure around the tip profile of the main blades of M6237 and the SRV4. The lip shock of M6237 is significantly lower than that of the SRV4.

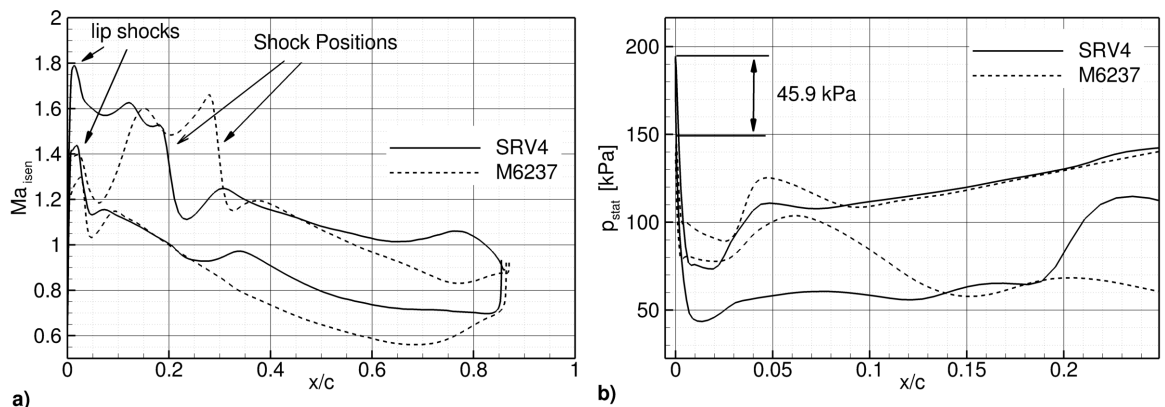


Figure 7: Distribution of the isentropic Mach number a) and the static pressure b) around the profile of the leading edges at the tip of the main blades of the reference member SRV4 and M6237.

Thus, the magnitude of the shock pressure pulse decreases which is shown in Fig. 7b.

Figure 8a illustrates the shock waves traveling with the impeller rotation through the inlet duct against the flow direction. These shock waves are the source of the blade tone noise in the far field, which is the strongest component of the sound emitted by transonic centrifugal compressors.

In Fig. 8a, it can be seen that the shock amplitudes seem to rise with increasing distance from the source location after an initial damping. The reason for this is that in Fig. 8a, fluctuations of the static pressure are presented. A conical, 58 mm long spinner is located in front of the leading edges of the main blades, as can be seen in Fig. 4. This spinner narrows the cross section so the flow velocity increases and the static pressure decreases.

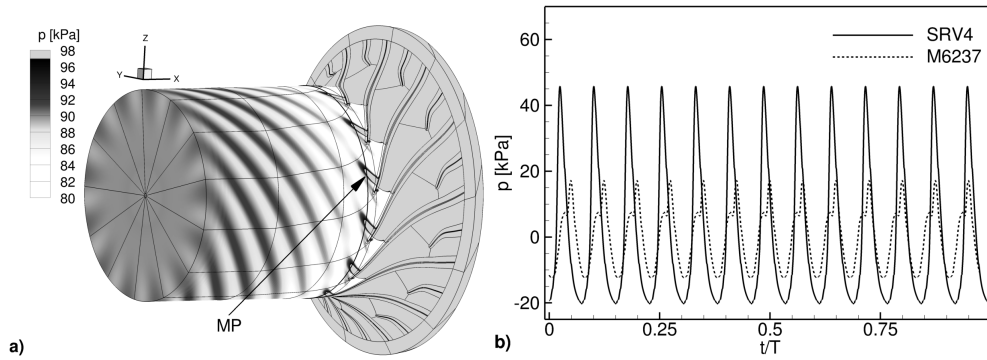


Figure 8: a) Pressure waves propagating in the inlet duct due to shocks in front of the leading edges b) Pressure fluctuations at the blade tip, directly in front of the leading edge (signed with “MP” in the left Figure) for one revolution of both members, SRV4 and M6237.

Figure 8b shows the pattern of the fluctuation of the static pressure at the blade tip, along a line near the leading edge (signed with “MP” in Fig. 8a) of both members, SRV4 and M6237. The peaks of the pressure pulses of M6237 are significantly lower than those of the reference Member SRV4. It is expected that the noise in the far field of the Member M6237 is lower than the noise of the reference compressor.

The splitter blades of the optimized members are shorter than those of the reference member, e.g. for M6237 they are shortened by approximately 37 %. Figure 9 shows the Mach number distribution of two planes, the impeller outlet plane and a parallel plane in the diffuser 10 mm downstream of the first plane. A comparison between the members SRV4 and M6237 is shown. The regions with lower flow velocity in both planes of M6237 are not as distinct as in SRV4.

For the reference member SRV4 the splitter blades are positioned exactly in the middle of the flow channel between two main blades. Mainly, they should relieve the main blades aerodynamically. The new splitter blades are designed in their geometry and positioning in the flow channel to reduce distinctive jet-wake or separation areas, to homogenize the outlet flow of the impeller, which leads to higher efficiencies and larger stall margins. The rake angle of the main blade of member M6237 is increased about  $28.4^\circ$  compared to the SRV4 and reached the limit defined in the optimization process. The rake angle of the independent parameterized splitter blades, however, only slightly increased. Fig. 9 shows that the outflow of the optimized member M6237 is more homogeneous compared to the initial member SRV4. Therefore, it was chosen the operating points of peak efficiency of both members. In this context, the values of the Mach number are not interesting.

The contribution of the angles of the rake and the trailing edges to the homogenization of the outlet flow will still be analyzed in detail and published in the future.

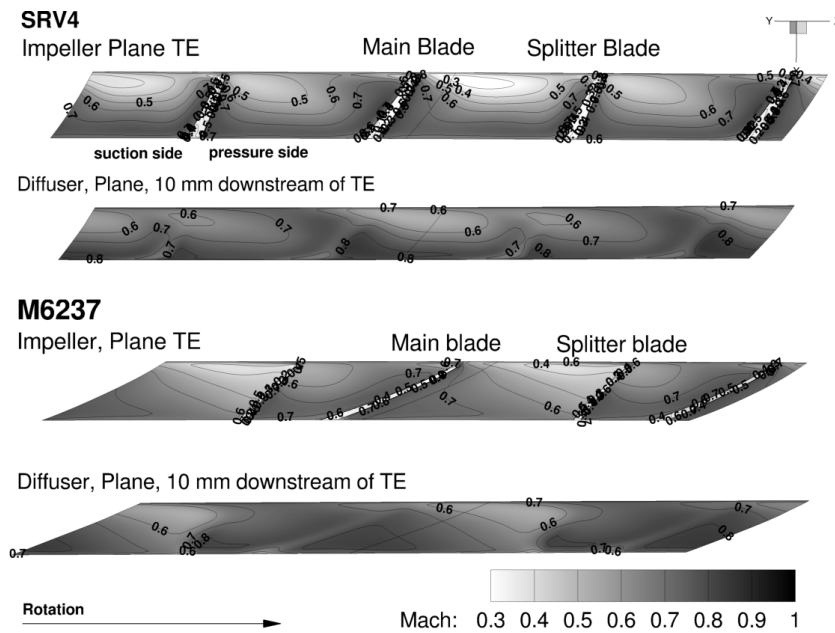


Figure 9: Diffuser flow: Mach number at impeller outlet plane and at diffuser plane 10 mm downstream of the trailing edges - comparison between the reference member SRV4 and M6237.

## CONCLUSIONS

This paper deals with the optimization of the performance of a centrifugal impeller performed with help of an automated procedure. The evolutionary optimizer developed at DLR, called AutoOpti, is used.

The main goals of the optimization are to increase the isentropic efficiency and extend the operating range at the design speed of 50,000 rpm, which are formulated as objective functions. The SRV4, the initial member, is the last numerically and experimentally tested impeller of the SRV series of DLR. To ensure the comparability of the optimization results with the previous members of the SRV series and the compatibility to the SRV test rig the inlet and outlet radius, the axial length and the number of blades as well as the design speed were not varied. A further goal of the optimization is to reduce the strongest component of the compressor noise in transonic regime, the shock induced blade tone noise.

The optimization was performed at three operating points on the design speed line with 45 free parameters.

Three representative members of the pareto front were selected to demonstrate the success of the optimization. The isentropic efficiency of the impeller is increased by 1.9 percentage points but the operating range could not be significantly increased.

The achieved values of the efficiencies are very good optimization results.

The shape of the leading edge of the main blades is very important for the performance, especially for the efficiency of the impeller. Due to the forward sweep of the leading edges in the tip region the shock shifts further downstream on the suction side. The lip shock decreases and thereby the efficiency increases. Also the blade tone noise is reduced.

The shortened splitter blades and their positioning inside the flow channel between two main blades contribute to the increase in efficiency and the enhancement of the operating range.

## OUTLOOK

In the following optimization phase, it will be aimed to maintain the efficiency improvement or trade the efficiency improvement against a better operation range.

Therefore, the mass flow difference between OP0 and OP1 of the optimization should be increased so that the distances of all operating points will be increased. That could lead to an increase of the operating range at the expense of efficiency.

The numerical evaluation of the mechanical characteristics of optimized radial impellers is part of future research at DLR.

## ACKNOWLEDGMENT

We would like to thank the DLR, Energy Programme Directorate for its support.

## REFERENCES

**Becker, K., Heitkamp, K., Kügeler, E.** (2010): *Recent Progress In A Hybrid-Grid CFD Solver For Turbomachinery Flows*, Proceedings Fifth European Conference on Computational Fluid Dynamics ECCOMAS CFD 2010. V European Conference on Computational Fluid Dynamics ECCOMAS CFD, 2010.

**Bräunling, W.J.G.**(2002): *Flugzeugtriebwerke*, Springer-Verlag, Berlin, Heidelberg 2002.

**Casey, M., Gersbach, F.** (2008): *An Optimization Technique For Radial Compressor Impellers*, Proceedings of ASME Turbo Expo 2008: Power for Land, Sea and Air GT2008 , Berlin, Germany, June 9 - 13, 2008.

**Cumpsty, N. A.** (1989): *Compressor Aerodynamics*, Longman Group UK Limited, Essex 1989.

**Kaplan, B., Nicke, E., Voss, C.** (2006): *Design of a Highly Efficient Low Noise Fan for Ultra-High Bypass Engines*, Proceedings of ASME Turbo Expo 2006: Power for Land, Sea and Air GT2006, Barcelona, Spain, May 8 - 11, 2006.

**Krain, H., Hoffmann, B.** (2005): *Homogene Lauf- /Leitradströmung im Radialverdichter; Abschlussbericht über das Vorhaben Nr. 798 (AiF-Nr. 13228NI)*, Technical Report Forschungsvereinigung für Verbrennungskraftmaschinen, Informationstagung Turbinen der FVV, Cologne, Issue R 532, 2005.

**Persigehl, B., Haag, J.-Ch., Verbaere, H., Hönen, H., Jeschke, P.** (2011): *Analysis of a Standard Turbocharger Application in Chemical Process Engineering*, Conference Proceedings Vol.1 of the 9th European Conference on Turbomachinery, Fluid Dynamics and Thermodynamics 21 - 25 March 2011, Istanbul, Turkey, 2011.

**Raitor, T.** (2010): *Experimentelle Ermittlung dominanter Schallquellmechanismen von Radialverdichtern*, Forschungsbericht 2010-04, Deutsches Zentrum für Luft- und Raumfahrt, Institut für Antriebstechnik, Fan und Verdichter, Köln, 2010.

**Siller, U., Voss, C., Nicke, E.** (2009): *Automated Multidisciplinary Optimization of a Transonic Axial Compressor*, 47th AIAA Aerospace Sciences Meeting Including The New Horizons Forum and Aerospace Exposition 5 - 8 Januray, Orlando, Florida, U.S.A., 2009.

**Siller, U., Aulich, M.** (2010): **Multidisciplinary 3D-optimization of a fan stage performance map with consideration of the static and dynamic rotor mechanics**, ASME Turbo Expo 2010, GT2010-22792, June 14-18, 2010, Glasgow, UK.

**Van den Braembussche, R. A.** (2000): *Radial Impeller Design Methology*, Course Note 162, von Karman Institute for Fluid Dynamics, Brussels Belgium, 2000.

**Van den Braembussche, R. A., Alsalihi, Z., Verstraete, T., Matsuo, A., Ibaraki, S., Sugimoto, K., Tomita, I.** (2012); *Multidisciplinary Multipoint Optimization of a Transonic Turbocharger Compressor*, Proceedings of ASME Turbo Expo 2012, GT2012-69645, June 11-15,

2012, Copenhagen, Denmark.

**Voss, C., Nicke, E.** (2008): *Automatische Optimierung von Verdichterstufen*, DLR-Forschungsbericht, Köln 2008.

**Yagi, M., Shibata T., Nishida, H., Kobayashi, H., Tanaka, M., Sugimura, K.** (2010): *Optimizing a Suction Channel to Improve Performance of a Centrifugal Compressor Stage*, Proceedings of ASME Turbo Expo 2010: Power for Land, Sea and Air GT2010-23019, June 14-18, 2010, Glasgow, UK.